Carbohydrate Polymers 83 (2011) 808–812

Contents lists available at ScienceDirect

Carbohydrate Polymers

journal homepage: www.elsevier.com/locate/carbpol

Carbon-13 CP/MAS solid state NMR and X-ray diffraction spectroscopy studies on lime wood decayed by *Chaetomium globosum*

Carmen-Mihaela Popescu[a,*], Per Tomas Larsson[b], Cornelia Vasile[a]

[a] *Romanian Academy "P. Poni" Institute of Macromolecular Chemistry, Department of Physical Chemistry of Polymers, 41A Gr. Ghica Voda Alley, Ro.700487, Iasi, Romania*
[b] *Innventia AB, Box 5604, SE-114 86 Stockholm, Sweden*

ARTICLE INFO

Article history:
Received 6 July 2010
Received in revised form 6 August 2010
Accepted 23 August 2010
Available online 27 August 2010

Keywords:
Biodegradation
X-ray diffraction
CP/MAS ^{13}C NMR spectroscopy

ABSTRACT

The degradation of the plant cell wall by microorganisms has been studied by X-ray diffraction, and solid state CP/MAS ^{13}C NMR spectroscopy. Lime wood (*Tilia cordata* Miller) samples were inoculated with *Chaetomium globosum* for various durations up to 133 days.

Structural modifications were assessed by comparing decayed lime wood samples with reference. These methods proved to be able to give insights into the modifications at a molecular level of the cell wall components by *Ascomycetes* fungi attack.

Significant changes in relative crystallinity and apparent lateral crystallite size, as measured by XRD, were detectable relatively early in the decay process. The content of hemicelluloses and cellulose in the wood samples decreased after biodegradation with *Chaetomium globosum*. The main chemical changes in wood during decay are the loss of hemicelluloses and cellulose simultaneously with lesser changes in lignin structure, which mainly consist in partial loss of methoxyl groups and Cα–Cβ bond cleavage and loss of β-O-4 linkages.

1. Introduction

Wood biodegradation is a relatively slow natural process carried out by specific microorganisms, mainly fungi (Eriksson, Blanchette, & Ander, 1990).

The main components of woody cell walls – cellulose, hemicelluloses and lignin – are degraded by various groups of organisms to different extents. Both the so-called soft rot and brown rot fungi, belonging to the *Ascomycetes* and *Basidiomycetes* respectively, principally decompose the polysaccharides. A third group, also *Basidiomycetes* and known as white rot fungi attack both the lignin and the polysaccharides either simultaneously or successively.

Although there are similarities in the chemical changes associated with soft rot and brown rot, the effects of these two types of decay on the cell wall morphology are quite different. Soft rot fungi occur preferably in hardwoods; where the hyphae penetrate mainly into the cell wall and develop a characteristic decay pattern as the well known chains of conically tipped cavities within the S2 layer. The attack in soft rot is definitely restricted to the neighborhood of the hyphae (Alves da Silva et al., 2007; Henriksson, Johansson, & Pettersson, 2000; Mohebby & Militz, 2010).

Decay results from the activities of enzymes, secreted by the fungal hyphae, acting on specific cell wall components. In soft rots the degradation is caused almost exclusively by polysaccharide splitting enzymes (Hammel, Kapich, Jensen, & Ryan, 2002; Kleist & Schmitt, 2001).

The complex mechanism of decay caused by these microorganisms has generated the necessity of looking into reliable analytical techniques able to provide information at a molecular level on the modifications produced on the cell wall components by microbial activity. Two non-invasive techniques that can potentially provide such information without laborious sample preparation (i.e. extraction) are X-ray diffraction and the solid state nuclear magnetic resonance spectroscopy.

X-ray diffraction (XRD) provides direct investigation into structure and is a widely used method to measure the microfibrillar helical angles of wood cells, since it is rapid and simple as compare to many other methods. Also XRD, which detects the interference pattern created when X-rays encounter the regularly spaced crystalline cellulose planes in wood, has been used for decades as a rapid method to observe the crystalline portion of wood, and is one of the primary tool used in the determination of the conformation and structure of cellulose microfibrils (Bhattacharya, Germinario, & Winter, 2008; Bootten, Harris, Melton, & Newman, 2008; Cunha, Freire, Silvestre, Pascoal Neto, & Gandini, 2010; Elanthikkal, Gopalakrishnapanicker, Varghese, & Guthrie, 2010; He, Tang, & Wang, 2007; Mihranyan, Llagostera, Karmhag, Stromme, & Ek, 2004; Rosa et al., 2010).

* Corresponding author. Tel.: +40 232217454; fax: +40 232211299.
E-mail address: mihapop@icmpp.ro (C.-M. Popescu).

0144-8617/$ – see front matter © 2010 Elsevier Ltd. All rights reserved.
doi:10.1016/j.carbpol.2010.08.049

Several studies have been reported on the application of carbon-13 cross-polarization/magic angle spinning (CP/MAS) NMR spectroscopy to structural studies of the cell wall and its isolated components. The attention has been focused on cellulose isolated from the other cell wall components, in particular on its crystalline and non-crystalline forms, as these two forms can be distinguished in CP/MAS spectra of isolated cellulose (Gilardi, Abis, & Cass, 1995) while the structure of native wood has raised less interest. Unfortunately, in the wood studies the necessary steps of isolation or fractionation may cause significant modifications in the wood structure. An essential advantage of solid state NMR spectroscopy is that samples can be studied in their native state without components' isolation or fractionation, and all chemical changes in the structure that may occur by chemical treatment are thereby avoided (Wikberg, 2004).

In this article we report further studies on the application of XRD and high-resolution, solid state CP/MAS ^{13}C NMR methods to characterize and gain insights on the molecular modifications of cell wall of lime wood (*Tilia cordata* Mill.), after biodegradation by soft rot *Chaetomium globosum*. In this we have taken advantage of the assignments of the signals made on isolated constituents (Atalla, Gast, Sindorf, Bartuska, & Maciel, 1980; Earl & VanderHart, 1980; Hatfield, Maciel, & Erbatur, 1987; Kolodziejski, Frye, & Maciel, 1982; Maciel, O'Donnell, Ackerman, Hawkins, & Bartuska, 1981) to identify resonances in intact cell walls that can act as quantitative markers for changes occurring during biodegradation. We wish to emphasize that all the measurements reported here are of samples of wood that have only been ground prior to recording the spectra; no extraction or separation of the individual components has been performed.

2. Experimental

2.1. Materials

Lime wood samples were cut from a tree with a age of 70 years from 1.30 m height above ground and let to air-dry thoroughly (TAPPI T 257 cm-02). Wood blocks (50 mm × 50 mm × 3 mm) were oven-dried at 105 °C (TAPPI T 264 cm-97), until constant weight was reached. The samples were sterilized and exposed (by contact method) to *C. globosum* in petri dishes containing 2% malt extract, 2% dextrose, 2% agar, in distilled water, pre-inoculated 1 week prior to the test and then they were incubated at 28 °C for 133 days.

By visual observation it has been established that the growing period of fungus on the surface of wood sample was of about 28 days; then the fungus reached the maturity and forms the spores and its attack is much aggressive. Visual aspect of the fungus colony on the surface of wood is the same for samples kept during period from 70 to 133 days.

During a 133-day period, at each 7-day interval, three lime wood samples were taken up from the agar medium. Mycelia were removed from their surfaces by repeated washings with twice-distilled water. Then the samples were oven-dried to constant weight. The mass losses of individual samples were calculated, and used to determine mean weight percentage losses.

The fungus action was manifested by a continuous decrease in sample mass of 0.49 (w/w)%/day during the first 70 days, being slower (0.29 (w/w)%/day) in following 63 days. Average mass loss for lime wood blocks after 133 days of exposure to *C. globosum* was 50.4 (w/w)%.

2.2. Methods

The X-ray diffraction (XRD) analysis was performed on a Bruker diffractometer equipped with a Kristalloflex 760 sealed-tube copper anode generator, operated at 40 kV and 40 mA, and on a two-dimensional position-sensitive wire-grid detector (Bruker AXS) pressured with xenon gas. Collimation was effected by a graphite monochromator with a 0.8 mm pinhole. Data in the range of $2\theta = 2–45°$ was obtained using a sample-to-detector distance of 9 cm and an accumulation of 1200 scans. The samples were placed in sealed Mark-Röhrchen glass capillaries (Charles Supper) of 1.0 mm inner diameter. All diffractograms were processed by subtracting a baseline image obtained using an empty capillary tube. The two-dimensional image was then integrated over 180° to chart the intensity as a function of 2θ.

The recorded diffractograms were deconvoluted using Gaussian profiles by means of Grams/32 program (Galactic Industry Corp.). The reduced chi-squared value, for all deconvoluted curves was $\chi^2 \leq 0.1$. After deconvolution, several parameters can be calculated and compared e.g. the crystalline index, the apparent crystallite size, the proportion of crystallite interior chains and the mass fraction of cellulose in wood (Popescu et al., 2008).

Solid state CP/MAS ^{13}C NMR spectroscopy. High-resolution solid state ^{13}C NMR spectra were recorded at 7.04 T with cross-polarization/magic angle spinning (CP/MAS) in a Bruker Avance AQS 300 WB spectrometer. All powdered samples were packed uniformly in a zirconium oxide rotor. All measurements were performed at 289 ± 1 K. The MAS rate was 5 kHz. A double air-bearing probe was used. Acquisition was performed with a CP pulse sequence, using a 4.5 μs proton 90° pulse, 800 μs ramped (100–50%) falling contact pulse and a 2.5 s delay between repetitions. A TPPM15 pulse sequence was used for ^{1}H decoupling. Glycine was used for Hartman–Hahn matching procedure and as external standard for the calibration of the chemical shift scale relative to tetramethylsilane ($(CH_3)_4Si$). The data point of maximum intensity in glycine carbonyl line was assigned a chemical shift of 176.03 ppm. Integration of the spectral region was done by means of Grams/32 program (Galactic Industry Corp.)

3. Results and discussion

3.1. X-ray diffraction

Among wood components only cellulose is crystalline, the other polymers being non-crystalline. The free hydroxyl groups present in the cellulose macromolecules are likely to be involved in a number of intramolecular and intermolecular hydrogen bonds, which may give rise to various ordered crystalline arrangements. It is well-known that the natural form of cellulose – cellulose I or native cellulose – has a three-dimensional structure, which is highly complex and not yet completely resolved as a result of the coexistence of two distinct crystalline forms, cellulose I_α and I_β (Browning, 1971).

Fig. 1 shows the X-ray diffractograms of the reference (undecayed) and decayed lime wood samples. The band from the 22.3° 2θ reflection of the decayed wood samples becomes broader and decrease in the intensity profiles with the increase in exposure time.

In order to examine the intensities of the diffraction bands and to establish the crystalline and the amorphous areas more exactly, the diffractograms were deconvoluted using Gaussian profiles (Fig. 2).

Crystallographic planes are labeled according to the cellulose I structure as described by Sugiyama, Vuong, and Chanzy (1991). After deconvolution, five bands were observed, namely: the 14.8–14.9° 2θ reflection assigned to the (1 0 1) crystallographic plane, the 16.5–16.8° 2θ reflection, assigned to the (1 0 $\bar{1}$) crystallographic plane, the 18.7° 2θ reflection, assigned to amorphous phases, the 20.0° 2θ reflection, assigned to the (1 0 2) crystallographic plane, and the 22.3° 2θ reflection, assigned to the (0 0 2) or

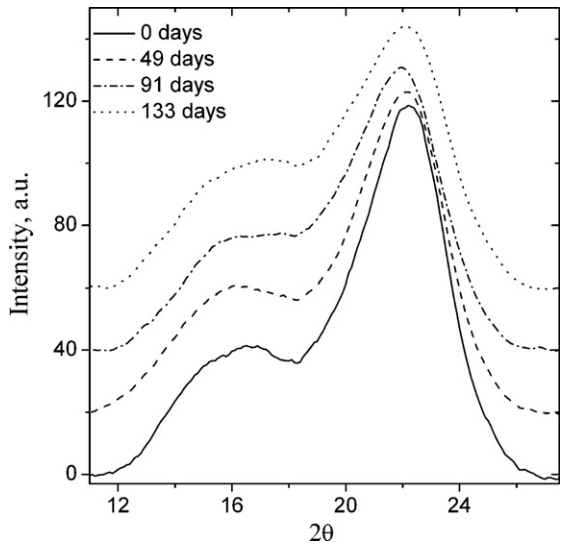

Fig. 1. X-ray diffractograms of reference and decayed lime wood samples.

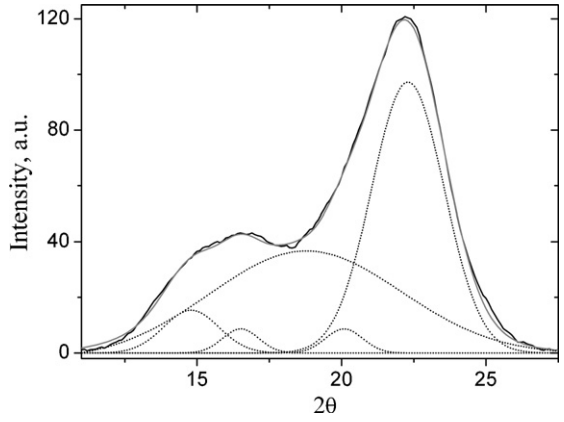

Fig. 2. Deconvoluted X-ray diffractograms of reference lime wood sample.

(2 0 0) crystallographic plane of cellulose I (Colom, Carrillo, Nogues, & Garriga, 2003; Silva et al., 2008) (Table 1).

The positions of the bands for the (1 0 1) and (1 0 $\bar{1}$) crystallographic planes were found to be slightly shifted to higher theta degrees in decayed lime wood compared to the reference lime wood sample (Table 1). The full width at half maximum of the diffraction bands increases after the degradation by fungi.

The degree of crystallinity of the reference and decayed wood samples was also estimated using FT-IR spectra (Popescu, Popescu, & Vasile, 2010) and the method proposed by Hulleman, van Hazendonk, and van Dam (1994). The ratio between the absorption intensities of the band at 1280 cm^{-1} (assigned to the C–H bending mode) and the band at 1200 cm^{-1} (assigned to the C–O–C stretching mode of the pyranose ring) ($R_{c,h} = I_{1280}/I_{1200}$) was used to determine

Table 1
The band positions of crystalline (cr) and amorphous (am) cellulose forms for the studied lime wood samples.

Sample	cr (1 0 1)	cr (1 0 $\bar{1}$)	am	cr (1 0 2)	cr (2 0 0)
0 days	14.79	16.51	18.75	20.08	22.29
28 days	14.81	16.63	18.73	20.05	22.27
49 days	14.82	16.71	18.74	20.09	22.23
70 days	14.85	16.72	18.75	20.07	22.25
91 days	14.90	16.84	18.72	20.05	22.28
112 days	14.93	16.83	18.75	20.05	22.27
133 days	14.92	16.85	18.73	20.03	22.25

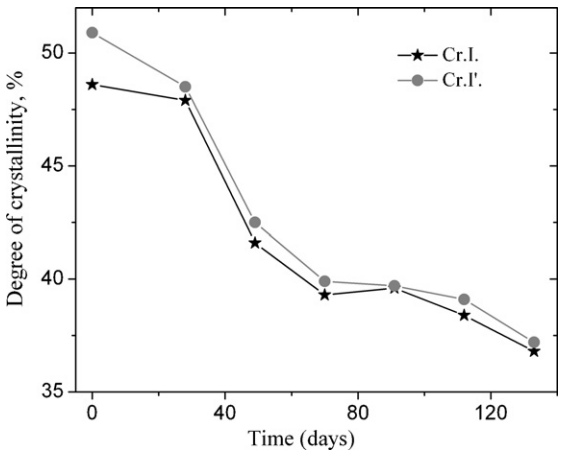

Fig. 3. Degree of crystallinity vs. exposure time for studied lime wood samples (Cr.I – crystallinity degree from XRD, Cr.I′ – cristallinity degree from FT-IR spectroscopy).

the degree of crystallinity for lime wood samples (Ilharco, Garcia, Lopes da Silva, & Ferreira, 1997). The degree of crystallinity (Cr.I. and Cr.I′) determined using both methods (XRD and FT-IR), was found to decrease as the biodegradation process advanced (Fig. 3 and Table 2). FT-IR determinations of the degree of crystallinity were in good agreement with those obtained by XRD measurements (Fig. 3).

It is known from X-ray crystallography that band broadening may be due to decrease in cellulose crystallite thickness, increase in packing defects, compositional inhomogeneity, the presence of very fine particles, etc. The decrease in the apparent crystallite size (L002 – Table 2) and in the proportion of crystallite interior chains (X – Table 2) of cellulose has been shown by other authors who suggested that this decrease arises from increased chain mobility caused by the degradation, permitting a higher percentage of the chains to move into the perfect register of the crystals. Correspondingly, the cellulose content decreases.

It is interesting to note that significant changes in relative crystallinity and apparent lateral crystallite size, as measured by XRD, are detectable relatively early in the decay process. It has been established that this is most likely due to extensive cellulose and hemicellulose depolymerization.

3.2. Solid state CP/MAS ^{13}C NMR spectroscopy

The solid state CP/MAS ^{13}C NMR spectroscopy has been extensively applied to the structural studies of natural wood. In native wood the main structural components, cellulose, hemicelluloses, lignin and, to some extent, extractives, give their characteristic shifts to the spectrum (Atalla et al., 1980; Bardet, Foray, & Trân, 2002; Bootten et al., 2008).

A characteristic of the CP/MAS ^{13}C NMR of wood is the broadening of most signals due to the unordered molecular structure of lignin and hemicelluloses and partly cellulose. Relatively sharp

Table 2
The calculated parameters for the studied lime wood samples.

Parameters	Cr.I.	Cr.I′	L200 (nm)	X	Cell. content
0 days	48.6	50.9	3.19	0.41	69.43
28 days	47.9	48.5	3.17	0.41	68.43
49 days	41.6	42.5	3.07	0.39	59.43
70 days	39.3	39.9	3.01	0.38	56.14
91 days	39.6	40.7	2.89	0.37	56.57
112 days	38.4	39.1	2.86	0.36	54.86
133 days	36.8	37.2	2.81	0.35	52.57

Cr.I′ – degree of crystallinity calculated from FT-IR spectra, L – apparent crystal size, X – proportion of crystallite interior chains.

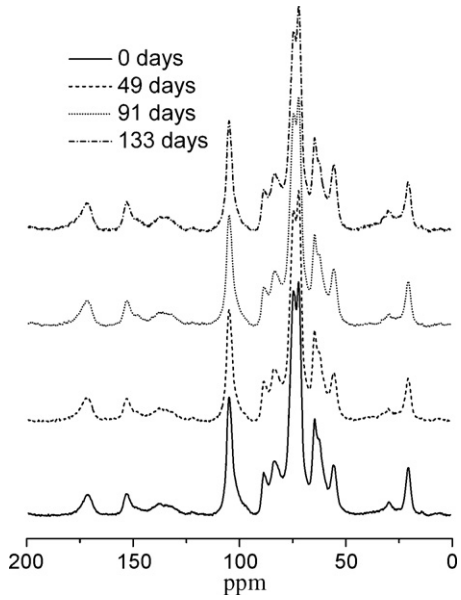

Fig. 4. CP/MAS ^{13}C NMR spectra of reference and biodegraded lime wood samples.

signals are assigned to ordered cellulose or hemicelluloses, while broader background signals are assigned to lignin and disordered hemicelluloses (Earl and VanderHart, 1980; Gilardi, Abis, & Cass, 1995; He, Tang, & Wang, 2007; Larsson, Wickholm, & Iversen, 1997).

The corresponding CP/MAS ^{13}C NMR spectra of the reference and three representative lime wood samples biodegraded by *C. globosum* are shown in Fig. 4.

The chemical shift assignments of the NMR spectra of the wood samples were made on the basis of literature data (Bardet, Foray, & Trân, 2002; Larsson, Wickholm, & Iversen, 1997; Wickholm, Larsson, & Iversen, 1998) and the outcome is reported in Table 3. There are no differences between chemical shifts in the reference and decayed wood spectra.

Conventional CP/MAS ^{13}C NMR measurements followed by signal integration of the reference and decayed wood samples have been carried out to obtain information of the chemical changes due to the fungal decay.

Differences in relative signal intensities could be observed as the biodegradation process advanced. In particular, in the aliphatic region of spectra in Fig. 4, the intensities of the signal at 105 and 89 ppm corresponding to cellulose resonances are altered by the biodegradation. It was difficult to determine whether the cellulose or the hemicelluloses components were more affected because of the overlapping signals.

Table 3
Resonance assignment of CP/MAS ^{13}C NMR spectra of reference and decayed lime wood.

Assignments	Chemical shift (ppm)	
	Reference	Decayed
Carboxyl groups of hemicelluloses	171.6	171.4
S3(e), S5(e) in lignin	153.1	153.0
S3(ne), S5(ne), G1, G4 in lignin	148.6	148.4
S1(e), S4(e), G1(e) in lignin	137.7	137.2
S1(ne), S4(ne), G1(e) in lignin	134.1	133.9
G6 in lignin	122.6	121.4
C1 carbon of cellulose	104.9	104.9
Shoulder of C1 carbon of hemicelluloses	101.6	101.4
C4 carbon of crystalline cellulose	88.6	88.5
C4 carbon of non-crystalline cellulose	83.2	83.4
C2,3,5 of cellulose	74.6	74.6
C2,3,5 of cellulose, lignin	72.2	72.1
C6 carbon of crystalline cellulose	64.7	64.7
C6 carbon of non-crystalline cellulose	62.4	62.6
Aryl methoxyl carbons of lignin	55.9	55.7
	29.8	30.2
CH_3 in acetyl groups of hemicelluloses	20.6	20.9

S – syringyl, G – guaiacyl, e – etherified, ne – nonetherified.

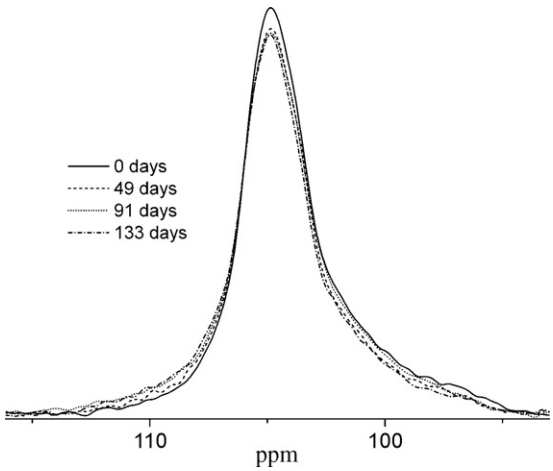

Fig. 5. CP/MAS ^{13}C NMR spectra of reference and biodegraded lime wood samples in the 115–90 ppm region.

However, by observing the shoulder at 101.6 ppm assigned to C1 carbons of hemicelluloses, it could be noted that its intensity was reduced (Fig. 5). The biodegradation of hemicelluloses reduced the broad background contribution to the aliphatic part of the spectrum, and it may have been responsible for the apparent sharpening of some signals in this region.

Also the signal at 105.2 ppm assigned to the C-1 of cellulose decreases with increasing exposure time.

After integrating the area of the 112–93 ppm region, it decreased with increased exposure time from 13.7 to 12.5% (Table 4). This is consistent with the removal of hemicelluloses and also the transformation of crystalline cellulose in non-crystalline cellulose during exposure to soft rot fungus. Also the slight decrease in resolution of the signal at 88.6 ppm (as compared to that at 83.3 ppm) upon fungal degradation suggested that the fungus had removed the crystalline cellulose in preference to the non-crystalline cellulose. This interpretation is supported by the presence of a small decrease in spectral resolution in the 93–80 ppm region after decay (Table 4).

Reference and decayed lime wood, gave distinct signals at 55.8 ppm from aryl methoxyl carbons of lignin, the percentage contribution of methoxyl C to the total pool of carbons from the NMR spectra increased 5.6% in reference wood to 7.2% upon fungal decay (Table 4). The resonances between 158 and 112 ppm are from car-

Table 4
Composition of lignocellulosic substrates in reference and decayed lime wood exposed to soft-rot fungi as obtained from integration of CP/MAS ^{13}C NMR spectra.

Area	Sample			
	0 days	49 days	91 days	133 days
COO– (177–165 ppm)	3.44	4.19	4.56	4.83
C-3/C-5 of S (158–145 ppm)	3.16	3.47	3.57	4.14
C-1/C-4 of S (145–125 ppm)	3.34	3.76	3.64	4.19
Aromatic C	6.50	7.23	7.21	8.30
C-1 (112–93 ppm)	13.74	13.48	13.08	12.53
C-4 (93–80 ppm)	10.92	10.87	10.79	10.41
C-2, 3, 5 (80–67.5 ppm)	41.11	40.99	40.26	38.77
C-6 (67.5–58.5 ppm)	14.06	13.57	13.56	13.29
O-alkyl-C	79.83	78.91	77.69	75.44
$-OCH_3$ in lignin (58.5–48 ppm)	5.61	5.65	6.60	7.20
alkyl-C (30.3–29.7 ppm)	1.12	0.56	0.58	1.14
CH_3 (25–16 ppm)	3.46	3.45	3.33	3.47

bon in aromatic rings from lignin. These are increasing from 6.5 to 8.3% after 133 days of exposure. One plausible explanation is that there has been an overall increase in lignin content, which could elevate the amount of aromatic rings and methoxyl groups in the altered wood relative to polysaccharides.

However, a sharpening in the aromatic and methoxy resonances manifested by the samples treated with *C. globosum* may indicate a higher degree of mobility gained by a modified, but still polymeric lignin. This could correspond to the enzymatically liberated lignin known to be produced by these fungi.

The degradation of wood was accompanied by an increase and broadening in the resonance at 171.6 and 20.6 ppm, corresponding to carbonyl and carboxyl groups and their attached methyl groups, as these are known to be the oxidation products of cell wall structures, especially an increase of carbonyl groups in lignin.

Comparing these results obtained from the two methods, it appears that the main chemical changes in wood during decay due to soft-rot are loss of hemicelluloses and cellulose simultaneously with lesser changes in lignin structure, mainly loss of methoxyl groups and Cα–Cβ bond cleavage and loss of β-O-4 linkages.

Wood softening is the main feature of decay caused by soft rot fungi. Causative agents of soft rot are largely represented by ascomycetous and imperfect fungi. The absolute content of lignin in wood specimens affected by these fungi is not changed significantly. Compared to basidiomycetes, soft rot fungi are not as adapted to degrading lignin. They release a variety of hydrolases, which cleave structural polysaccharides of cell walls, and oxidoreductases, which act both on carbohydrate components of wood (glucose oxidases, galactose oxidases, and CDHs) and phenolic compounds (peroxidases and laccases). Chaetomium is the best-known producers of cellulose–hemicellulase systems.

4. Conclusions

In this study, XRD and solid state CP/MAS ^{13}C NMR spectroscopy were used to examine qualitative and semi-quantitative changes in the components of soft-rot decayed wood.

Significant changes in relative crystallinity and apparent lateral crystallite size, as measured by XRD, are detectable relatively early in the decay process. This is most likely due to extensive cellulose and hemicellulose depolymerization.

Solid state ^{13}C CPMAS NMR spectroscopy results showed that the relative content of hemicelluloses and cellulose in the wood samples decreased after biodegradation with *C. globosum*. It appears that the main chemical changes in wood during decay due to soft-rot are the loss of hemicelluloses and cellulose simultaneously with lesser changes in lignin structure, mainly some loss of methoxyl groups and Cα–Cβ bond cleavage and loss of β-O-4 linkages.

References

Alves da Silva, C., Bacellar Monteiro, M. B., Brazolin, S., Carballeira Lopez, G. A., Richter, A., & Brag, M. R. (2007). Biodeterioration of brazilwood *Caesalpinia Echinata* Lam. (Leguminosae–Caesalpinioideae) by rot fungi and termites. *International Biodeterioration and Biodegradation*, *60*, 285–290.

Atalla, R. H., Gast, J. C., Sindorf, D. W., Bartuska, V. J., & Maciel, G. E. (1980). Carbon-13 NMR spectra of cellulose polymorphs. *Journal of the American Chemical Society*, *102*, 3249–3251.

Bardet, M., Foray, M. F., & Trân, Q. K. (2002). High-resolution solid-state CPMAS NMR study of archaeological woods. *Analytical Chemistry*, *74*, 4386–4390.

Bhattacharya, D., Germinario, L. T., & Winter, W. T. (2008). Isolation, preparation and characterization of cellulose microfibers obtained from bagasse. *Carbohydrate Polymers*, *73*, 371–377.

Bootten, T. J., Harris, P. J., Melton, L. D., & Newman, R. H. (2008). WAXS and ^{13}C NMR study of *Gluconoacetobacter xylinus* cellulose in composites with tamarind xyloglucan. *Carbohydrate Research*, *343*, 221–229.

Browning, B. L. (1971). *Encyclopedia of polymer science and technology*. New York: John Wiley and Sons.

Colom, X., Carrillo, F., Nogues, F., & Garriga, P. (2003). Structural analysis of photodegraded wood by means of FTIR spectroscopy. *Polymer Degradation and Stability*, *80*, 543–549.

Cunha, A. G., Freire, C. S. R., Silvestre, A. J. D., Pascoal Neto, C., & Gandini, A. (2010). Preparation and characterization of novel highly omniphobic cellulose fibers organic–inorganic hybrid materials. *Carbohydrate Polymers*, *80*, 1048–1056.

Earl, W. L., & VanderHart, D. L. (1980). High resolution, magic angle spinning carbon-13 NMR of solid cellulose I. *Journal of American Chemical Society*, *102*, 3251–3252.

Elanthikkal, S., Gopalakrishnapanicker, U., Varghese, S., & Guthrie, J. T. (2010). Cellulose microfibres produced from banana plant wastes: Isolation and Characterization. *Carbohydrate Polymers*, *80*, 852–859.

Eriksson, K. E. L., Blanchette, R. A., & Ander, P. (1990). *Microbial and enzymatic degradation of wood and wood components*. Berlin: Springer.

Gilardi, G., Abis, L., & Cass, A. E. G. (1995). Carbon-13 CP/MAS solid-state NMR and FT-IR spectroscopy of wood cell wall biodegradation. *Enzyme and Microbial Technology*, *17*, 266–275.

Hammel, K. E., Kapich, A. N., Jensen, K. A., Jr., & Ryan, Z. C. (2002). Reactive oxygen species as agents of wood decay by fungi. *Enzyme and Microbial Technology*, *30*, 445–453.

Hatfield, G. R., Maciel, G. E., & Erbatur, G. (1987). Qualitative and quantitative analysis of solid lignin samples by carbon-13 NMR spectrometry. *Analytical Chemistry*, *59*, 172–179.

He, J., Tang, Y., & Wang, S. Y. (2007). Differences in morphological characteristics of bamboo fibres and other natural cellulose fibres: Studies on X-ray diffraction. Solid state ^{13}C-CP/MAS NMR, and second derivative FTIR spectroscopy data. *Iranian Polymer Journal*, *16*, 807–818.

Henriksson, G., Johansson, G., & Pettersson, G. (2000). A critical review of cellobiose dehydrogenases. *Journal of Biotechnology*, *78*, 93–113.

Hulleman, S. H. D., van Hazendonk, J. M., & van Dam, J. E. G. (1994). Determination of crystallinity in native cellulose from higher plants with diffuse reflectance fourier transform infrared spectroscopy. *Carbohydrate Research*, *261*, 163–172.

Ilharco, L. M., Garcia, A. R., Lopes da Silva, J., & Ferreira, L. F. V. (1997). Infrared approach to the study of adsorption on cellulose: Influence of cellulose crystallinity on the adsorption of benzophenone. *Langmuir*, *13*, 4126–4132.

Kleist, G., & Schmitt, U. (2001). Characterisation of a soft rot-like decay pattern caused by *Coniophora puteana* (Schum.) Karst in Sapelli Wood (Entandrophragma cylindricum Sprague). *Holzforschung*, *55*, 573–578.

Kolodziejski, W., Frye, J. S., & Maciel, G. E. (1982). Carbon-13 NMR spectrometry with CP/MAS for analysis of lodgepole pine wood. *Analytical Chemistry*, *54*, 1419–1424.

Larsson, P. T., Wickholm, K., & Iversen, T. (1997). A CP/MAS ^{13}C NMR investigation of molecular ordering in celluloses. *Carbohydrate Research*, *302*, 19–25.

Maciel, G. E., O'Donnell, D. J., Ackerman, J. J. H., Hawkins, B. H., & Bartuska, V. J. (1981). A carbon-13 NMR study of four lignins in the solid and solution states. *Makromolecular Chemistry*, *182*, 2297–2304.

Mihranyan, A., Llagostera, A. P., Karmhag, R., Stromme, M., & Ek, R. (2004). Moisture sorption by cellulose powders of varying crystallinity. *International Journal of Pharmaceutics*, *269*, 433–442.

Mohebby, B., & Militz, H. (2010). Microbial attack of acetylated wood in field soil trials. *International Biodeterioration and Biodegradation*, *64*, 41–50.

Popescu, C.-M., Tibirna, C. M., Raschip, I. E., Popescu, M.-C., Ander, P., & Vasile, C. (2008). Bulk and surface characterization of unbleached and bleached softwood kraft pulp fibres. *Cellulose Chemistry and Technology*, *42*, 525–547.

Popescu, C.-M., Popescu, M.-C., & Vasile, C. (2010). Characterization of fungal degraded lime wood by FT-IR and 2D IR correlation spectroscopy. *Microchemical Journal*, *95*, 377–387.

Rosa, M. F., Medeiros, E. S., Malmonge, J. A., Gregorski, K. S., Wood, D. F., Mattoso, L. H. C., Glenn, G., Orts, W. J., & Imam, S. H. (2010). Cellulose nanowhiskers from coconut husk fibers: Effect of preparation conditions on their thermal and morphological behavior. *Carbohydrate Polymers*, *81*, 83–92.

Silva, M. C., Lopes, O. R., Colodette, J. L., Porto, A. O., Rieumont, J., Chaussy, D., et al. (2008). Characterization of three non-product materials from a bleached eucalyptus kraft pulp mill, in view of valorising them as a source of cellulose fibres. *Industrial Crops and Products*, *27*, 288–295.

Sugiyama, J., Vuong, R., & Chanzy, H. (1991). Electron diffraction study on the two crystalline phases occurring in native cellulose from an algal cell wall. *Macromolecules*, *24*, 4168–4175.

Wickholm, K., Larsson, P. T., & Iversen, T. (1998). Assignment of non-crystalline forms in cellulose I by CP/MAS ^{13}C NMR spectroscopy. *Carbohydrate Research*, *312*, 123–129.

Wikberg, H. (2004). *Advanced solid state NMR spectroscopic techniques in the study of thermally modified wood*. Academic Dissertation. Helsinki.